# Relationships Between Emission Sources and Airmass Characteristics in East Asia during the TRACE-P Period

G. Kurata[1], G. R. Carmichael[2], T. Kitada[1], Y. Tang[2], J.-H. Woo[2], N. Thongboonchoo[2]

1. Department of Ecological Engineering, Toyohashi University of Technology, Toyohashi, Japan

2. Center for Global and Regional Environmental Research, University of Iowa, Iowa, USA

Revised : May 5, 2003

**Abstract:**

Long-range transport of the pollutants influenced by both anthropogenic and natural emission source in East Asia including the biomass burning emission in Southeast Asia was investigated by using the backward trajectory analysis from NASA TRACE-P flight tracks and a numerical simulation with three-dimensional chemical transport model (STEM-2k1). 5-days backward trajectory from flight track was calculated every 5 minutes. To make clear the relationship between the observed airmass and their source region, the observed and calculated concentration were allocated to the 1° x 1° mesh where the corresponding backward trajectory passed over, and the average value and the average bias between observed and modeled concentration were calculated for each mesh. As a result, we found systematic features of the spatial distribution for each species. In this period, observed concentration of CO and some NMHCs and the ratios between these species were highly associated with the feature of emission source distribution and their regional characteristics. Reconstructed field of the observed and modeled ratio between CO and NMHCs, such as ethane/CO and ethane/propane, by the backward trajectory could well reproduce the emission ratio of East Asia. We also investigated the time rate of change of the concentration of species and their ratio along the trajectory. From this analysis, the propane/ethane ratio and propane/acetylene ratio were proved to keep their emission ratio during regional transport. From the backward trajectory analysis, we also found the fact that our emission quantities from biomass burning have still some error for specific hydrocarbons. Further investigation will improve the model accuracy and potential capacity. As a case study, we also investigated the systematic difference of propane vs. acetylene/CO ratio found between the model and observation. The analysis is shown to explain that possible reason of the difference is the emission factor of the biomass burning. This kind of

analysis may help to determine the emission factor by observation-based inventory scheme.

Keyword: Chemical transport model, Trajectory Analysis, Emission inventory, Biomass burning, Tropospheric composition

## 1. Introduction

Due to the rapid development of East Asia, pollutant levels have increased, and the impacts of long-range transport of pollution on northern Pacific region and North America are of growing concern. These pollutants alter the tropospheric chemical composition, and they may affect a wide range of the phenomena from acid rain in East Asia to the global climate change. (*Phadnis et al*, 2000)

TRACE-P was an aircraft observation campaign organized by NASA during February to April 2001. In this campaign, two aircraft, a DC-8 and a P-3B, observed a large number of gas-phase and aerosol species and meteorological and optical properties, with the goal to clarify the contribution of the anthropogenic pollution to the tropospheric chemical composition of the northern Pacific. Fig.1 shows the flight tracks of both aircraft over which data was collected.

We applied a chemical transport model in forecast-mode to support the aircraft flight planning and the design of the observation strategies, and in post-analysis mode to interpret the observed data (*Carmichael, et al*, 2003). Emission inventories were developed to support this experiment (Streets et al., and Woo et al., 2003). Even though a large amount of effort has been made to improve the accuracy of these emissions, the uncertainty is still very large, especially in the developing countries, and for specific categories such as domestic fuel use.

There are two types of the method to estimate emission distributions and intensities, i.e., bottom-up and observation-based. The bottom-up scheme is commonly used to make regional or global emissions, and this method constructs the inventories using sectional and regional statistics on fuel usage, economic activity, etc.. To evaluate this scheme, comparison between observation and the calculated result of the model that used these inventory are usually used. The observation-based (sometimes referred to as top-down) scheme is based on the observation dataset and backward trajectories from the location of the observation. These techniques

are sometimes very useful, when the species are inert and time-independent. However, generally it is difficult to estimate accurate distribution of the source from this scheme, because there are many factors that affect the concentration of the species, such as transport, diffusion and mixing of the airmass, chemical reaction and deposition, etc.

In this study, we use a hybrid method that combines both bottom-up and observation-based method. We first use the bottom-up emission data for the model calculation, and applied the backward trajectory analysis along with the observed values quantify differences between model calculated and observed values. In this way we identify systematic errors in the bottom-up inventory, and suggest ways that this information can be used improve the emission inventories.

## 2. Method

### 2.1. Chemical Transport Model

We use the STEM-2k1 chemical transport model (*Tang et al*, 2003) to simulate trace species distributions for this period. The CTM was driven by the meteorological field calculated by CFORS/RAMS model, which used the ECMWF reanalysis data (6 hours interval, 1° x 1° horizontal resolution) for initial and boundary conditions (Uno et al., 2003)

The chemical mechanism of STEM-2k1 is based on the SAPRC 99 (*Carter,* 2000), which consists of 93 species and 225 reactions. Also this version is incorporated with on-line calculation of the photolysis rates, considering the influences of cloud, aerosol and gas-phase absorptions due to $O_3$, $SO_2$ and $NO_2$, using the NCAR Tropospheric Ultraviolet-Visible (TUV) radiation model (*Madronich,* 1999). Details regarding the radiative transfer calculations are presented in *Tang et al*. (2003). Boundary conditions were selected based on observational data.

The emission data used in this calculation is based on *Streets et al.,* and *Woo et al.,* (2003). It is a bottom-up inventory driven by regional-specific information on fuels and activity from various economic sectors (e.g., domestic, transport, power generation, industrial). This emission inventory includes all anthropogenic source, biomass burning, volcanoes and biogenic source. Lightning $NO_x$, dust and sea salt

emission were estimated within the on-line CFORS framework *(Uno et. al.* 2003). The model domain is shown in Fig. 1. The horizontal grid size is 80km, and the vertical domain was divided into 23 layers up to 23km.

### 2.2. Backward trajectory analysis

In this study, the 5-minute merged dataset of the TRACE-P observation for both the DC-8 and P-3B aircraft was used for the whole analysis and comparison with the model calculation. We calculated, using the 3-dimensional RAMS meteorological fields, 5 days backward trajectories every 5-minutes along the flight paths. The location of the start point of each trajectory corresponds to the defined location of the 5-minute merged dataset of the observation. The number of trajectories calculated was 2300. We also extracted the calculated concentration of each species, meteorological parameter, and photolysis rate along each trajectory from the three-dimensional model output. We used the observed data and extracted data from model output along the flight track and trajectories to reconstruct the horizontal and 3 dimensional information, and compared these with the emission information.

## 3. Result

### 3.1. Model performance

Fig. 2 shows the model performance in the form of scatter plots between model and observations, for all flight tracks for selected species. For most species the data are within a factor 2, except for $NO_x$. For CO and NMHCs there was good agreement with the observations. In the following analysis we use the CO and NMHC data in the analysis of the relationships between emission source regions and characteristics of the observed airmass.

The reason why the model always underestimates CO and NMHCs at high concentration is due to the model resolution. The model couldn't reproduce the narrow dense plume from coastal megacitis. Most of high concentration of CO was observed in the yellow sea, downwind of coastal megacities of China.

Model performance for each NMHCs is also different. The correlation coefficients (R values) between the model and observation within the lowest 1km for ethane and propane were 0.89 and 0.84, respectively for the DC-8 data. However, CO and acetylene have lower R values (0.76 and 0.68, respectively). This reflects the fact that the emissions of CO and acetylene arise from all types of combustion processes, many of which are highly uncertain in magnitude and/or in spatial/temporal distribution (e.g., biomass burning, domestic cooking and heating). (Carmichael et al., a,b, 2003).

### 3.2. Backward trajectories

Fig.3 shows statistics associated with the number of the trajectories that passed over each mesh (1° x 1°) for all flights. Fig. 3 (a) and (b) show that the count for the trajectories that passed under 1500m from the surface, and between 1500m and 3000m, respectively. We restricted the analysis to trajectories under 3000m for the following analysis, because these are the airmasses most likely to pick-up signals from the surface emissions. We see in the lower troposphere that airmases tend to come from the northwest, while for heights over 3000m airmass tend to come from the southwest. Unfortunately, the number of trajectories is very small from some region, such as northeastern part of India, Vietnam, and Cambodia. The grid cells with fewer than 5 trajectories were excluded from these figures. However many grid cells have a sufficient number of associated trajectories to estimate regional influences, including the biomass burning regions, such as northern Thailand and Myanmar.

### 3.3. Comparison of the concentration between model and observation

Fig. 4 shows the average observed concentration fields of CO, ethane, acetylene and propane reconstructed using the backward trajectories. The average concentration on each mesh is defined by following equation.

$$C = \frac{1}{N}\sum_{i}^{N} C_i \qquad (1)$$

Here, N is the number of the trajectories that passed over each mesh under 3000m above the ground. $C_i$

denotes the observed concentration on the airplane that is associated with the species back trajectory. Please note that the averaged concentration, C, does not include the atmospheric processing during transport from the location above mesh to the observed location.

Fig 4 (a) shows the average of observed CO calculated in this way. Very high averaged CO concentrations (>350ppbv) were seen for airmasses that passed over central China area and South East Asia. CO emissions in central China are very large both from industry and domestic use of biofuel and fossil fuel. During this time period, biomass burning in South East Asian was also a major source of CO. Furthermore, the relatively small average CO levels (100-150ppbv) were associated with airmasses from the Pacific Ocean.

Fig.4 (b) – (d) present the results for ethane, acetylene and propane, respectively. For the ethane and propane, there are large gradients from north to south. In the case of acetylene, we see high concentrations in the same areas as CO, but there is no significant north-south gradient.

Fig. 5 shows the bias between averaged observation and model calculation defined as following equation.

$$B = \frac{1}{N}\sum C_{i,\mathrm{mod}} - \frac{1}{N}\sum C_{i,\mathrm{obs}} \quad (2)$$

Here, B represents the bias between averaged observation and model calculation [ppbv], $C_{i,mod}$ is the calculated concentration of the species at the flight location [ppbv] , $C_{i,obs}$ is the observed concentration at same location. [ppbv]. So this value represents the systematic error of the CTM calculation.

In the case of CO, the model under-predicts values when the airmasses came from central China where the very high average CO concentration were observed. Under-predictions are also shown for airmasses from some parts of SEA. However, at other SEA regions, and locations near the west boundary, we over predict CO, and this may indicate that the boundary CO concentrations used for the southwest and west boundaries may be too high.

The bias for ethane and propane show similar feature. The model under predicts these species around Japan, Korea, and Northern China. One of the possible reasons is the underestimation of the boundary concentrations at the northern edge. Another possibility is that the emission intensity of hydrocarbon from Japan and Korea are underestimated. In the case of acetylene, the model calculation reproduced well the observed concentrations, except for airmasses that came from the central part of China and SEA. This seems

to be associated with the biomass burning emissions. However we cannot see the corresponding error in the bias for ethane and propane. Emission factors for biomass burning need further investigation.

From this kind of analysis, we identify model problems possibly associated with emission estimates.

### 3.4. Comparison of the ratio between model and observation

The ratios between the species are used in this section instead of the concentrations. Some of these ratios, such as acetylene/CO, have been suggested to be an indicator of atmospheric processing (*Smyth,* 1996) (*McKeen,* 1996), and they have wide range of variability of their values in emission factors. So, the combinations of these ratios will be useful to classify the airmass in terms of atmospheric processing and the relationship with emission source. In this case, we used the administrative districts instead of the latitude longitude mesh to compare with the emission inventory, because the statistics used in the emission inventory were mostly based on the administrative districts.

The left panel of the Fig. 6 (a) is a ratio of ethane to CO and ethane to propane, calculated from the emission estimates. Center and right panels are the regression slope between the same combination of species using the observations and model values, respectively. For this analysis, we also used the values at flight location and distributed by backward trajectory. Since CO and ethane have considerable background concentration, and they have wide range of spatial variation. So, we first subtracted the background concentration calculated from the relationship with potential temperature. Then, we calculated the slope by linear regression for the ratio.

In the case of the ethane/CO ratio, the observed ratio and model ratio are quite similar in terms of both spatial pattern and absolute value; the values are also consistent with the emission ratios in the northern regions. However the ratio for airmasses from SEA region are completely different from the emission ratio. One of the possible reasons is that because the most of airmass came from SEA was observed at high altitude, and the background CO in high altitude is very small. On the other hand, the vertical variation of the background concentration of ethane is not so large. So, the dilution of CO by the mixing with ambient air is controlling the ratio of ethane/CO for the airmass from SEA.

Another possible reason is the uncertainty of the emission factors from biomass burning include the

dynamically change of emission factor with the combustion conditions. Fig. 6 (b) shows the ratio of ethane/propane. In this case, the ratio from the observations are similar to the emission features, including the airmass from SEA. The ratio from model values also shows the same qualitative features. However, the spatial variation of the ratio is more uniform than that compared to the emission ratio.

### 3.5. Time rate of change of the concentration along the trajectories.

The analysis in the previous section imply that the model and observed values along the flight track. The change of the concentration along the trajectory was not considered. In the next analysis, we use extracted model values along the trajectory, including information of chemical reaction, diffusion, convective mixing, to help understand how ratios can change as air masses age.

Fig. 7 shows the averaged time rate of change of the calculated concentrations along the trajectories. Only the trajectories under 3000m are shown. For all species, the concentration increase over the land areas, especially over the high emission regions, and decrease over the ocean and at remote continental regions. Increasing on the ocean is mainly due to the mixing with more polluted airmass. The pattern is very similar for all species, however it is importance to identify the differences between each species. The increasing rate of CO over SEA is much larger than that over China. On the other hand, the increasing rate of the other hydrocarbon is similar value in both SEA and China.

### 3.6. Average time rate of change of the ratio of NMHCs and CO.

Fig. 8 shows the average time rate of the change of the ratios of propane/acetylene, propane/ethane and propane/CO. The time rate of change was calculated every 30 minutes on each backward trajectory by using the extracted model result, and allocated the value to the mesh where the airmass was located at that time. The increase phase of the ratio-change is associated with the regional emission ratios and the background ratios of the concentration. In the case of propane/CO, CO has a significant background concentration, so the background ratio of propane/CO is very small. So, over source regions, the ratio generally increases rapidly towards the value of the emission ratio. This same feature is shown for propane/ethane. On the other hand, at

remote areas, both species are generally decreased by chemical reaction with OH or mixing with cleaner air. In this case, the time rate of change of the ratio is determined by the reaction rate constant with the OH radical. The reaction rate of propane with OH is larger than that of CO, acetylene and ethane with OH. So, the ratios generally decrease.

Comparison of these three figures shows some interesting features. The propane/ethane ratio increases over both biomass regions and Chinese industrial regions. However, the propane/acetylene ratio increases over biomass burning regions, but decreases over China. In the case of propane/CO, the ratio increases over China, but decreases over biomass burning regions. These differences are due to the differences in emission factors for industry and biomass burning, and the resulting regional gradients in emission intensities. Whether the ratio increases or decreases at the first contact with the pollution source mainly depends on the background ratio. Because, initial and boundary concentration for the species that have very small background concentration is usually set to the unfounded small value in the model.

### 3.7. Vertical structure of the time rate of change of the ratio of NMHCs and CO

We also investigated the vertical structure of the time rate of change along the trajectory. Fig. 9 is a vertical structure of the time rate of change of the ratio of propane/acetylene, propane/ethane and propane/CO, respectively. These are averages of the values on all trajectories between 20°N-30°N, and for every 1km. For the propane/acetylene ratio, the values increase over biomass burning regions and decrease over China. These change over the source region depend on the background and emission ratios. An important feature of the change of the ratio is seen over remote areas (such as over the ocean). As shown the ratio of propane/acetylene decreases over the Pacific Ocean with a rate of ~ 0.002 [-/h], and this decrease is due to the reaction rate with OH and mixing with background airmasses. Reaction with OH decreases the ratio because the OH reaction of propane is slightly faster than that with acetylene. Fig. 9 (b) shows the change of propane/ethane ratio. In this case, the ratio decreases at remote areas, because the reaction rate of propane with OH is much larger than that of ethane. The average rate of decrease is about 0.001[-/h] in this case. The spatial variation of the emission ratio of propane/ethane ranges from 0.2 – 1.0. The time rate of change of the propane/ethane ratio is sufficiently small so that the emissions signal is during regional transport.

This time-rate of change of the ratio is very important to associate the airmass with specific source region. Especially, propane/ethane and propane/acetylene have wide variety of the ratio. So, considering the change of these ratios in the airmass is very important.

## 4. Case study – airmass characterization by the ratio – (Propane vs. acetylene/CO ratio)

Fig. 10 is a scatter plot of observed propane concentration against the observed acetylene/CO ratio (using all observation data points). Two relationships are identified from this figure. One relationship has a regression slope of ~ 400 [ppbv/-], the second has a slope of ~ 120 [ppbv/-]. To identify the difference of the characteristic of these two airmasses, further investigations were carried out.

Fig.11 shows scatter plots between propane and acetylene, the left panel is using the observations and the right panel is from the calculation values. The red points represent those points associated with high acetylene concentrations (>0.3ppbv) and large propane/acetylene ratios (>0.6) classified using the observation points. Comparison of the scatter plots for the observation and model calculation, shows that the model relationship between propane and acetylene is too uniform compare with the observation.

Fig. 12 (a)(b) are scatter plots between model and observation for acetylene and propane. From Fig. 12(a), it is clear that model underestimate acetylene concentration for the airmass classified by red points. This evidence means that our emission estimate for the region where these airmasses traveled over seems to have some problem.

Fig. 13 is the percentage of the trajectories for the segregated airmass, which is colored by red in Fig. 11 and 12. This figure shows that most of the airmass that has small propane/acetylene ratio tend to come from South East Asia region. One possibility of the reasonable emission source associated with these airmass is biomass burning. In the TRACE-P period significant biomass burning was observed in this region and we already identified the airmass which have high CO associated with biomass burning, and performed some test run for these emission (Tang, et. al., 2003 and Woo et. al., 2003).

We could identify the possible source for the discrepancy between model and observation by the backward trajectory analysis, and emission factor of acetylene for biomass burning need to be investigated more. However, further modification of the emission intensity must be coupled with bottom-up inventory to

assure the rationality.

## 5. Conclusion

We investigated the model capability for associating the observation airmass with source regions, using chemical transport model, STEM-2k1, and backward trajectory analysis framework. The CTM well reproduced the spatial and temporal distributions of ozone, CO and other NMHCs along the flight tracks.

We reconstructed the map of the average concentration and the bias between model and observation by using backward trajectory. From this analysis, we found that the observed very high CO concentration were always associated with central China and Southeast Asian in this period. And also found systematic under estimate of ethane and propane on the northern region and peculiar under estimate of acetylene for the airmass from SEA.

Backward trajectory analysis coupled with the observed ratio between CO, ethane, propane and acetylene could be compared with emission ratio. Observed ethane/propane ratio was well agreed with that of emission ratio. However, ratio of calculated ethane/propane showed too uniformity for all region.

Also, we investigated the time rate of change of the concentration of some NMHCs and their ratios. From the horizontal and vertical structure of these ratios, the propane/ethane ratio and propane/acetylene ratio were proved to keep their emission ratio during regional transport. And, their time rate of change was determined by the reaction rate with OH and mixing with background airmass.

From the backward trajectory analysis, we also found the fact that our emission quantities from biomass burning have still some error for specific hydrocarbons. Further investigation will improve the model accuracy and potential capacity.

As a case study, we also investigated the systematic difference of propane vs. acetylene/CO ratio found between the model and observation. The analysis is shown to explain that possible reason of the difference is the emission factor of the biomass burning. This analysis may help to determine the emission factor by top-down inventory scheme.

From these analysis coupled with backward trajectory, we could found many importance information associated with emission estimate. However, to make the systematic scheme to improve the emission estimate

could with this kind of analysis, further detail consideration is necessary.

**Acknowledgement**

This work was supported in part by the 21st Century COE Program "Ecological Engineering for Homeostatic Human Activities", from the ministry of Education, Culture, Sports, Science and Technology of Japan.

**Reference**

Carmichael, G. R., Tang, Y., Kurata, G., Uno, I., Streets, D.G., Woo, J.-H., Huang, H., Yienger, J., Lefer, B., Shetter, R.E., Blake, D.R., Atlas, E., Fried, A., Apel, E., Eisele, F., Cantrell, C., Avery, M.A., Barrick, J.D., Sachse, G.W., Brune, W.L., Sandholm, S.T., Kondo, Y., Singh, H.B., Talbot, R.W., Bandy, A., Thorton, D., Clarke, A.D., Heikes, B.G., 2003, Regional-Scale Chemical Transport Modeling in Support of Intensive Field Experiments: Overview and Analysis of the TRACE-P Observations, Journal of Geophysical Research, in press

Carmichael, G. R., Tang, Y., Kurata, G., Uno, I., Streets, D.G., Thongboonchoo, N., Woo, J.-H., Guttikundi, S., White, A., Wang, T., Blake, D.R., Atlas, E., Fried, A., Potter, B., Avery, M.A., Sachse, G.W., Sandholm, S.T., Kondo, Y., Talbot, R.W., Bandy, A., Thorton, D., Clarke, A.D., 2003, Evaluating Regional Emission Estimates Using The TRACE-P Observations, Journal of Geophysical Research, Submitted

Carter, W., 2000, Documentation of the SAPRC-99 chemical mechanism for VOC reactivity assessment, Final report to California Air Resources Board Contract No. 92-329, University of California Riverside

Madronich, S., Flocke, S., 1999, The role of solar radiation in atmospheric chemistry, in Handbook of Environmental Chemistry (P. Boule, ed.), Springer-Verlag, Heidelberg, 1-26

McKeen, S. A., Liu, S. C., Hsie, E.-Y., Liu, X., Bradshaw, J., Smyth, S. D., Gregory, G. L., Blake, D. R., 1996, Hydrocarbon ratios during PEM-WEST A: A model perspective, Journal of Geophysical Research, 101, 2087-2109

Phadnis, M. J., Carmichael, G. R., 2000, Transport and distribution of primary and secondary nonmethane volatile organic compounds in east Asia under continental outflow conditions, Journal of Geophysical Research, 105, 22,311-22,336

Smyth, S., Bradshaw, J., Sandholm, S., Liu, S., McKeen, S., Gregory, G., Anderson, B., Talbot, R., Blake, D., Rowland, S., Browell, E., Fenn, M., Merrill, J., Bachmeier, S., Sachse, G., Collins, J., Thornton, D., Davis, D., Singh, H., 1996, Comparison of free tropospheric western Pacific air mass classification schemes for the PEM-West A experiment, Journal of Geophysical Research, 101, 1743-1762

Street, D. G., Bond, T. C., Carmichael, G. R., Fernandes, S. D., Fu, Q., He, D., Klimont, Z., Nelson, S. M., Tsai, N. Y., Wang, M. Q., Woo, J.-H., Yarber, K. F., 2003, An inventory of gaseous and primary aerosol emissions in Asia in the year 2000, submitted to J. Geophysical Research

Tang, Y., Carmichael, G. R., Uno, I., Woo, J.-H., Kurata, G., Lefer, B., Shetter, R. E., Huang, H., Anderson, B. E., Avery, M. A., Clarke, T. D., Blake, D. R., 2003, Impacts of Aerosols and Clouds on Photolysis Frequencies and Photochemistry During TRACE-P, Part II: Three-Dimensional Study Using a Regional Chemical Transport Model, Journal of Geophysical Research, submitted

Uno, I., Carmichael, G. R., Streets, D. G., Tang, Y., Yienger, J. J., Satake, S., Wang, Z., Woo, J.-H., Guttikunda, S., Uematsu, M., Matsumoto, K., Tanimoto, H., Yoshioka, K., Iida, T., 2002, Regional Chemical Weather Forecasting using CFORS; Analysis of Surface Observation at Japanese Island Station during the ACE-Asia Experiment, submitted to J. Geophysical Research.

Woo, J.-H., Streets, D., Carmichael, G. R., Tang, Y., Yoo, B., Lee, W.-C., Thongboonchoo, N., Pinnock, S., Kurata, G., Uno, I., Fu, Q., Vay, S., Sachse, G. W., Blake, D. R., Fried, A., Thornton, D. C., 2003, The contribution of biomass and biofuel emissions to trace gas distributions in Asia during the TRACE-P Experiment, submitted to J. Geophysical Research

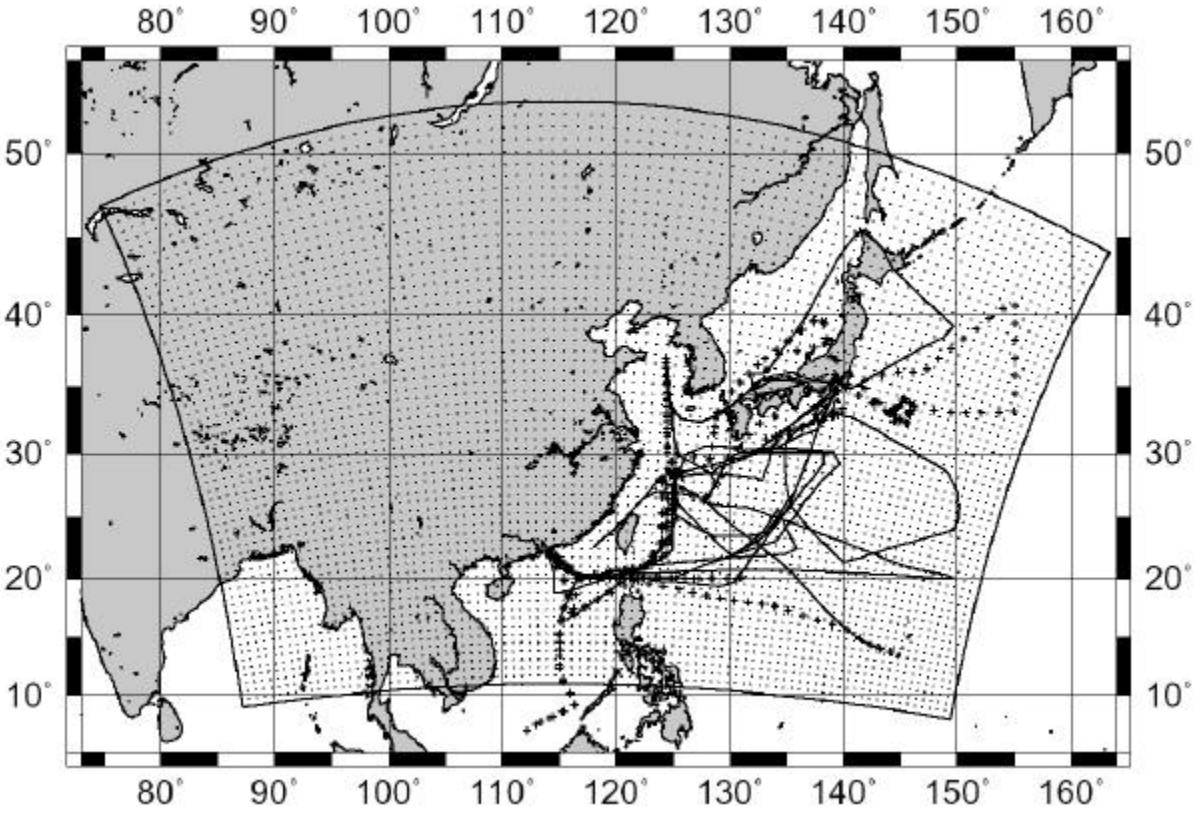


Fig.1 Flight track of each aircraft used in this analysis. Solid line represent DC-8 and Dashed line represent P3B. Our analysis use DC8 #6 - #17 and P3B #8 - #19. Internal box and points represent model boundary and grid point.

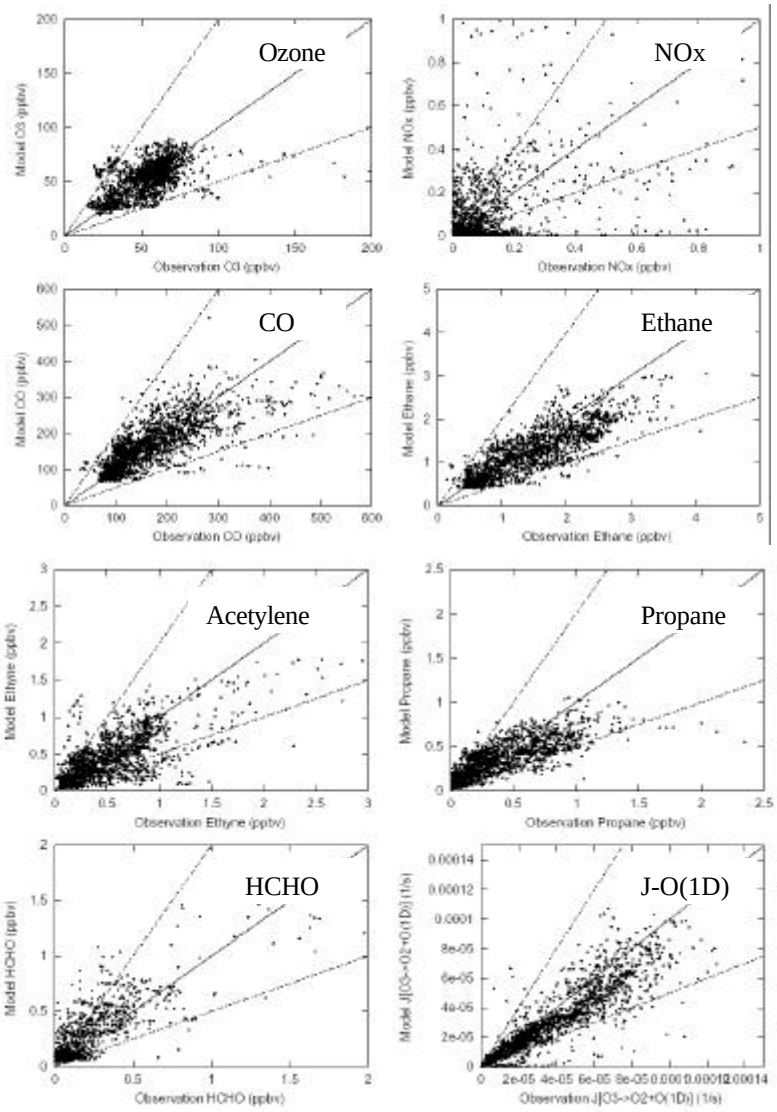


Fig. 2. Scatter plot between model and observed value at flight track every 5-minutes for both aircraft. Broken lines are represent factor 2.

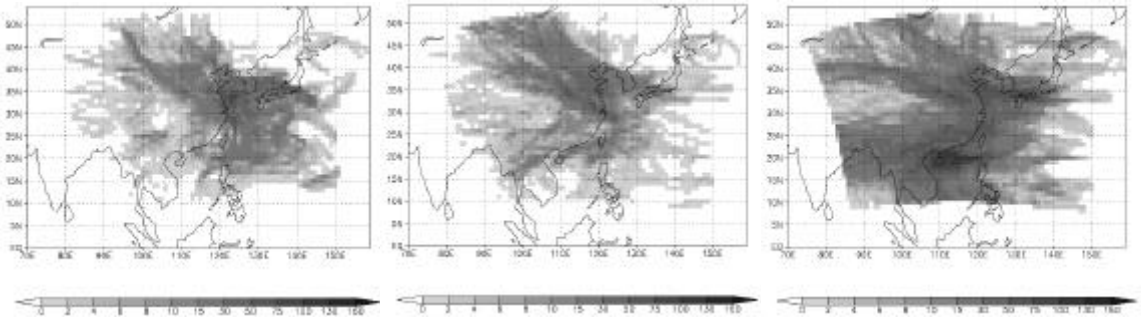

(a) 0 – 1500m (b) 1500 – 3000m (c) over 3000 m

Fig. 3. The total number of the trajectories that passed over each mesh (1° x 1°). Altitude is defined as the height about land-surface.

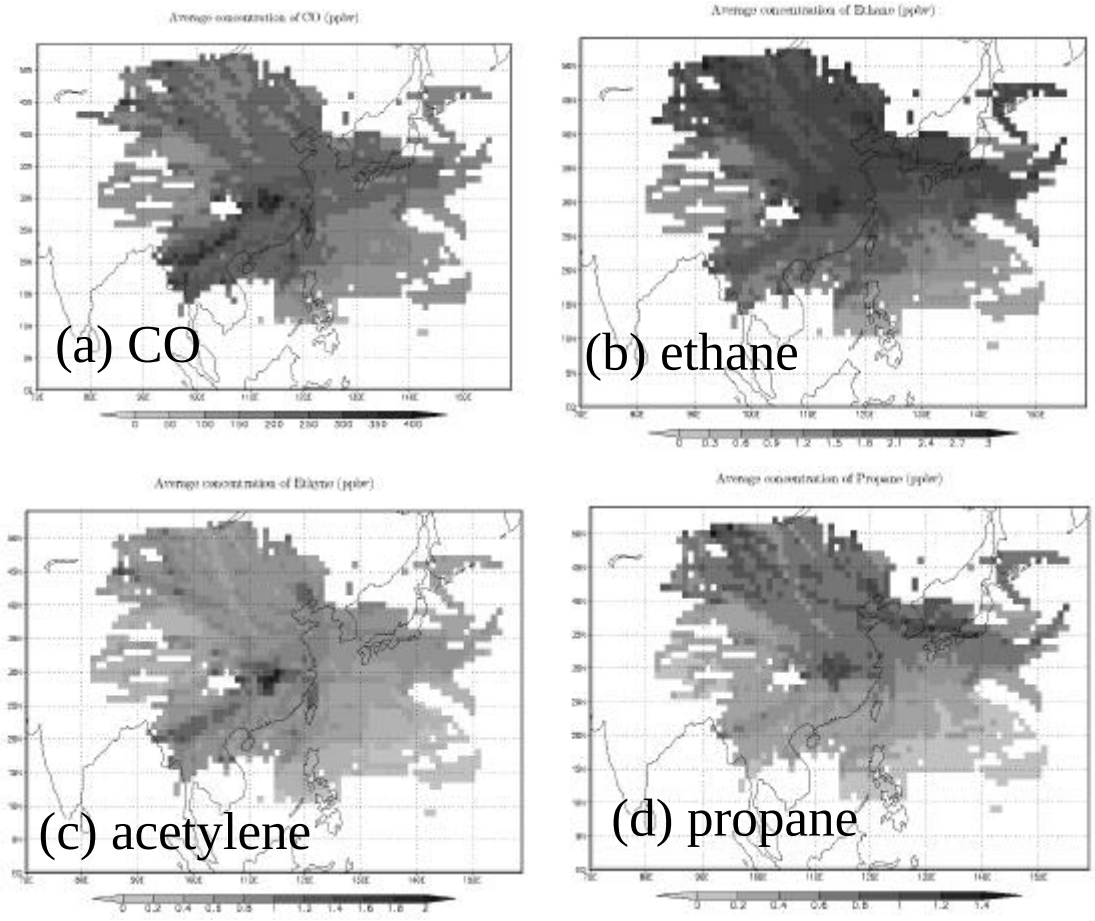


Fig. 4. Average field of the observed value reconstructed by backward trajectory. (a) CO, (b) Ethane, (c) Acetylene, (d) Propane (ppbv). All trajectories passed within 3000m of surface of each mesh were used.

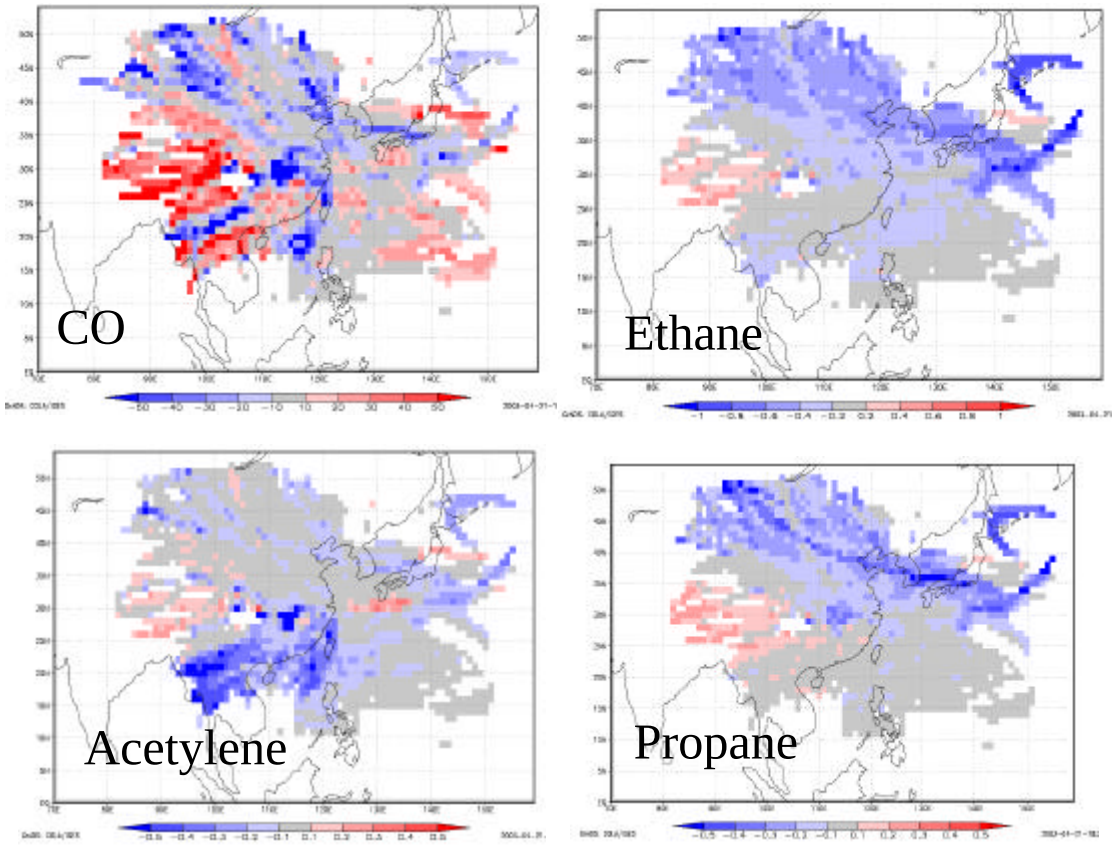


Fig. 5. Bias between the model and observation value reconstructed by backward trajectory for CO, Ethane, Acetylene and Propane, respectively. Plus values mean over-prediction, minus means under-prediction. All trajectories passed within 3000m of surface of each mesh were used.

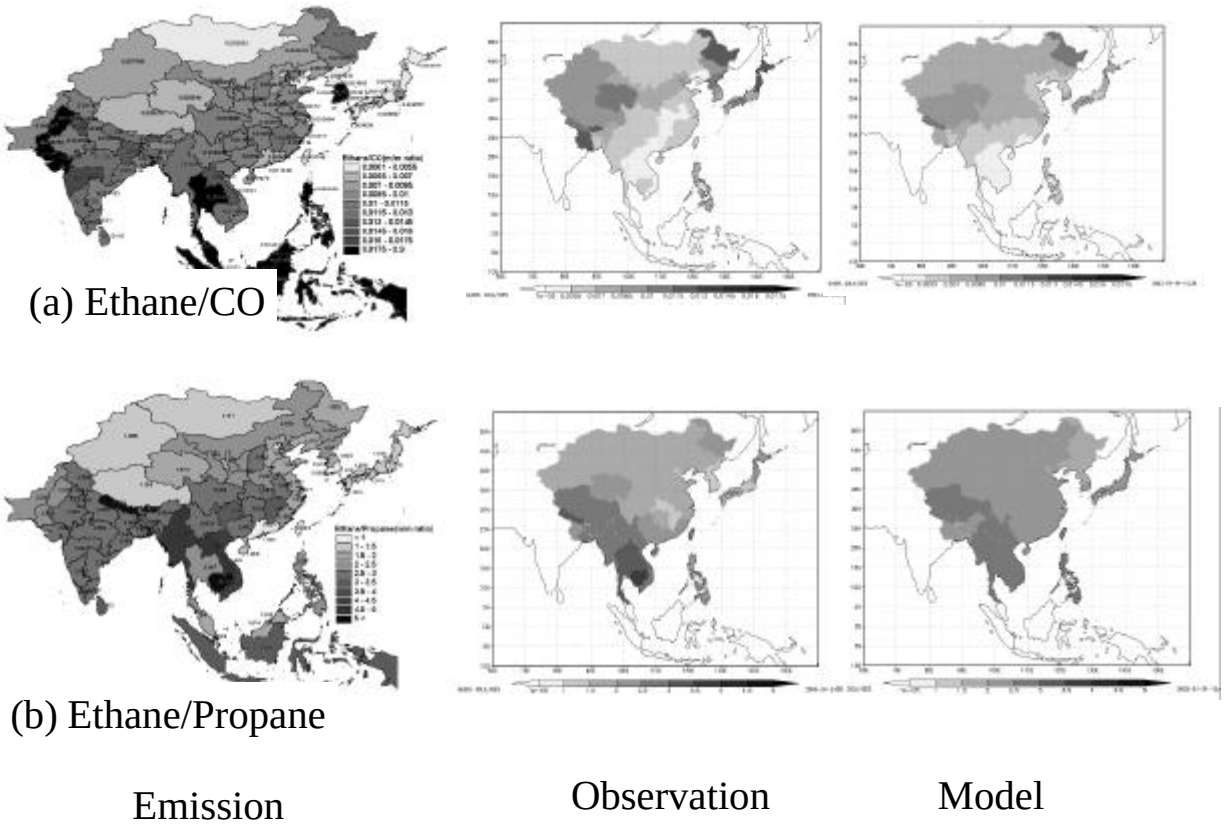


Fig. 6. Comparison of the ratio between model and observation by using backward trajectory to redistribute the value on flight track to the map. Ratios for observation and model are regression slope. Background concentration, which is a function of potential temperature, was subtracted for CO and ethane. All trajectories passed within 3000m of surface of each mesh were used.

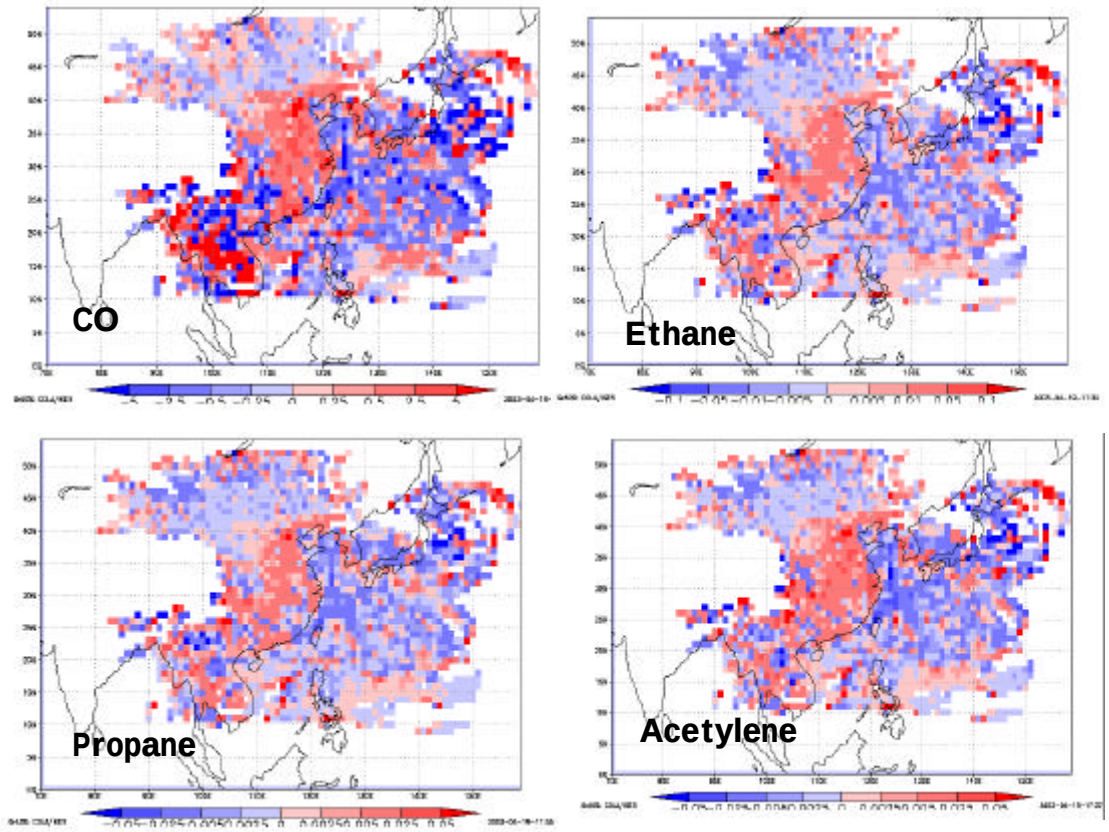


Fig. 7. Average of the time rate of change of the calculated concentration on the trajectories (ppbv $h^{-1}$). All trajectories passed within 3000m of surface of each mesh were used.

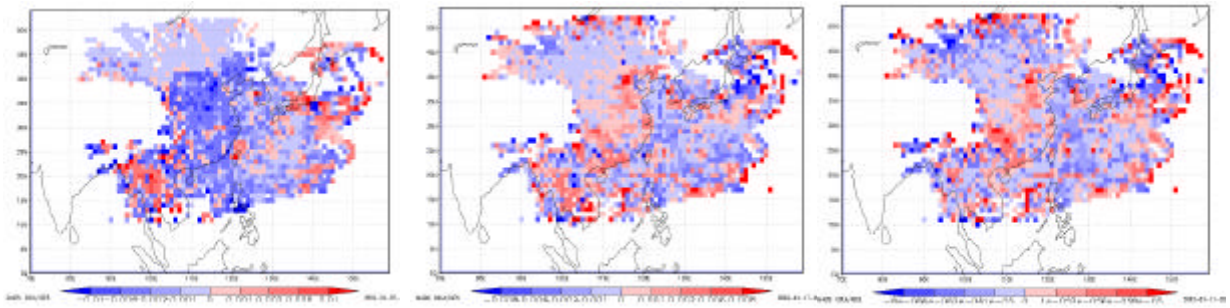


Fig. 8 Average time rate of the change of the ratio of Propane/Acetylene, Propane/Ethane and Propane/CO ($h^{-1}$). All trajectories passed within 3000m of surface of each mesh were used.

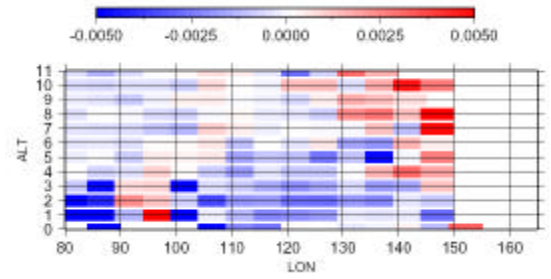


**(a) Propane/Acetylene [-/h]**

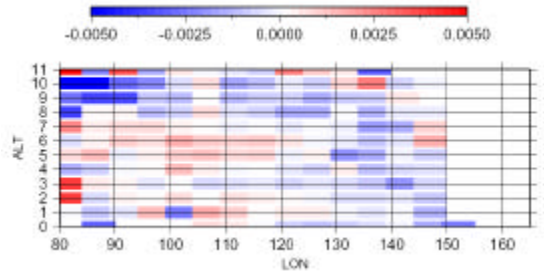


**(b) Propane/Ethane [-/h]**

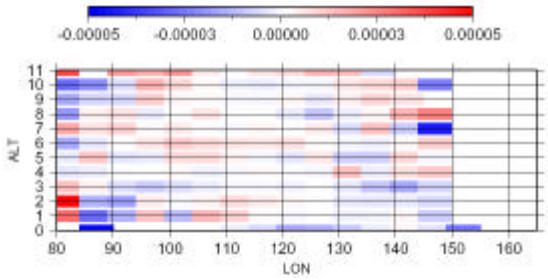


**(c) Propane/CO [-/h]**

Fig. 9. Vertical structure of the time-rate of change or the ratio of Propane/Acetylene, Peopane/Ethane and Propane/CO ($h^{-1}$). These are average of the value on the trajectories between 20°N-30°N.

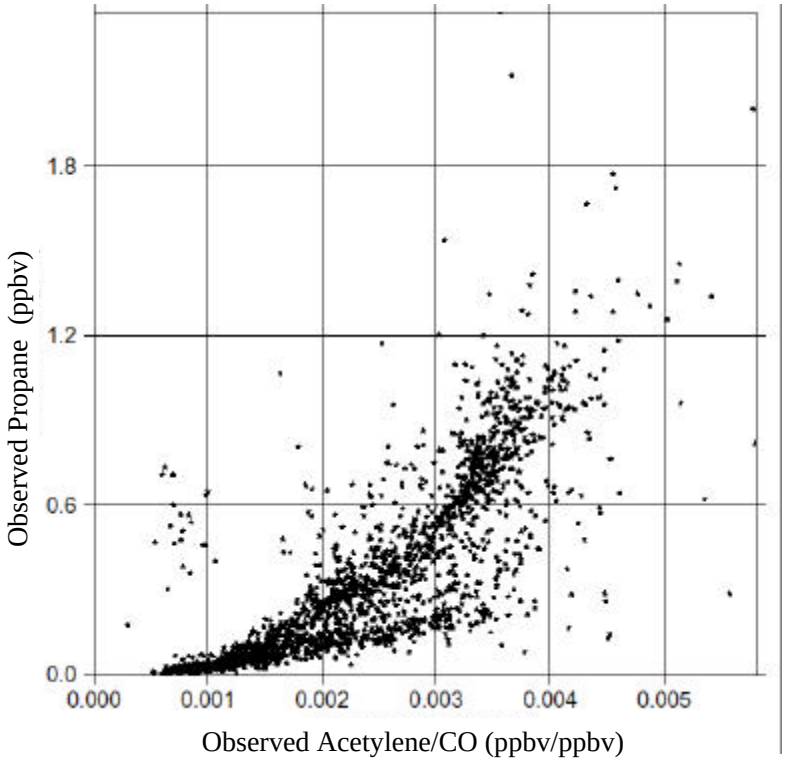


Fig. 10. Scatter Plot between Observed Propane and Observed Acetylene/CO ratio.

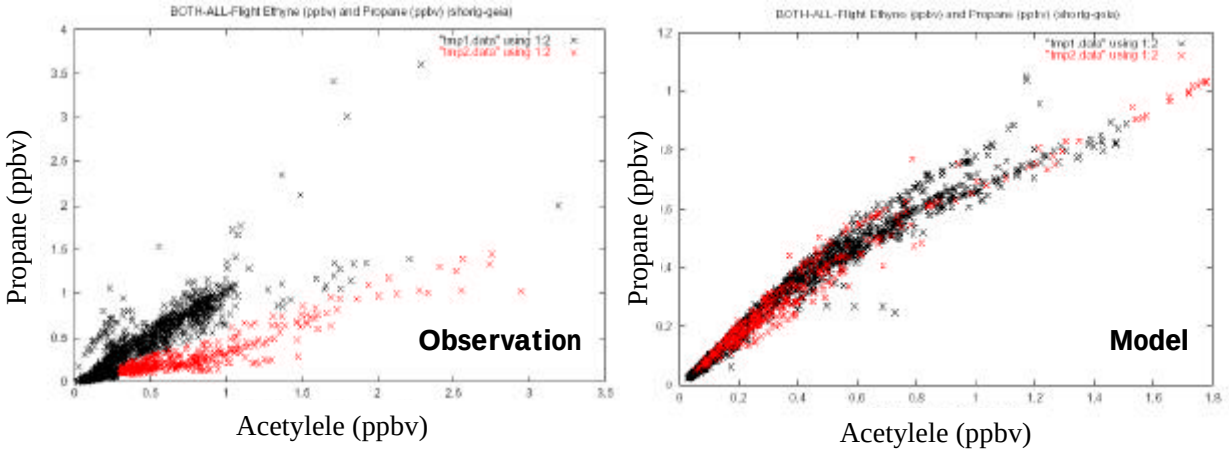


Fig. 11. Scatter plot between Propane and Acetylene both from Observation and Model.
Red point represent Acetylene > 0.3ppbv and Propane/Acetylene ratio > 0.6 within observation data.

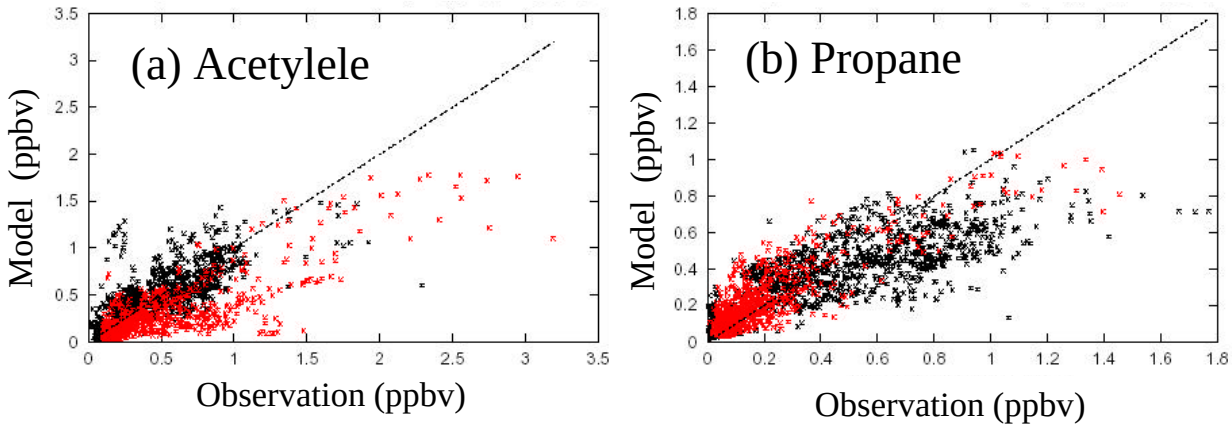


Fig. 12. Scatter plot between model and observation for Acetylene and Propane. Red color represents the same airmass in Fig. 11.

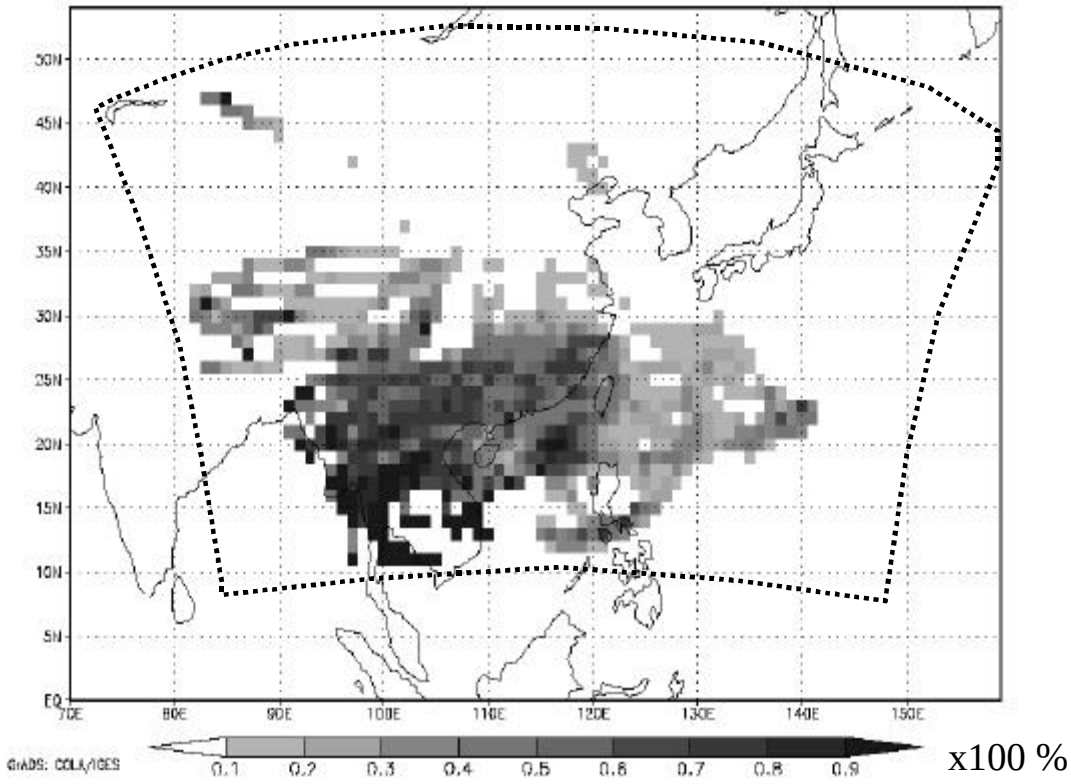


Fig. 13. The percentage of the trajectories, which is colored by red in Fig. 11 and 12 against all trajectories (x100 %). High percentage means that most of the airmass passed over that mesh were classified as having small propane/acetylene ratio.